Stress corrosion cracking induced by the combination of external and internal hydrogen in Al-Zn-Mg-Cu alloy

Tang, Jianwei
Department of Mechanical Engineering, Kyushu University

Wang, Yafei
Department of Mechanical Engineering, Kyushu University

Fujihara, Hiro
Department of Mechanical Engineering, Kyushu University

Shimizu, Kazuyuki
Department of Physical Science and Materials Engineering, Iwate University

他

出版情報：Scripta Materialia. 239, pp.115804-, 2024-01-15. Elsevier
バージョン：
権利関係：

Stress corrosion cracking induced by the combination of external and internal hydrogen in Al-Zn-Mg-Cu alloy

Jianwei Tang[a, *], Yafei Wang[a], Hiro Fujihara[a], Kazuyuki Shimizu[b], Kyosuke Hirayama[c], Kenichi Ebihara[d], Akihisa Takeuchi[e], Masayuki Uesugi[e], Hiroyuki Toda[a, *]

[a] Department of Mechanical Engineering, Kyushu University, Fukuoka 819-0395, Japan.

[b] Department of Physical Science and Materials Engineering, Iwate University, Iwate 020-8551, Japan.

[c] Department of Materials Science and Engineering, Kyoto University, Kyoto 606-8501, Japan.

[d] Center for Computational Science & e-Systems, Japan Atomic Energy Agency, Ibaraki, 319-1195, Japan.

[e] Japan Synchrotron Radiation Research Institute, Hyogo 679-5198, Japan.

Abstract

Stress corrosion cracking (SCC) behaviors induced by the combination of external and internal hydrogen (H) in an Al-Zn-Mg-Cu alloy were systematically investigated via *in situ* 3D characterization techniques. SCC of the Al-Zn-Mg-Cu alloy could initiate and propagate in the potential crack region where the H concentration exceeded a critical value, in which the nanoscopic H-induced decohesion of η-$MgZn_2$ precipitates resulted in macroscopic cracking. External H that penetrated the alloy from the environment played a crucial role during the SCC of the Al-Zn-Mg-Cu alloy by generating gradient-distributed H-affected zones near the crack tips, which made Al alloys in water environment more sensitive to SCC. Additionally, the pre-existing internal H was driven toward the crack tips during plastic deformation. It was involved in the SCC and made contributions to both the cracks initiation and propagation.

Keywords: Stress corrosion cracking; Hydrogen embrittlement; Al-Zn-Mg-Cu alloy; X-ray tomography; External and internal hydrogen

***Corresponding author**: Jianwei Tang

Affiliation: Department of Mechanical Engineering, Kyushu University, 744 Motooka, 27 Nishi-ku, Fukuoka-city, Fukuoka, 819-0395, Japan

E-mail address: tang.jianwei.299@m.kyushu-u.ac.jp

Al-Zn-Mg-Cu alloys are essential structural materials in the aerospace sector owing to their exceptional combination of high specific strength, superior formability and acceptable production cost [1]. Nevertheless, the susceptibility to stress corrosion cracking (SCC) can lead to catastrophic/premature failures of Al-Zn-Mg-Cu alloys under the synergistic effects of mechanical stress and the environment, which significantly challenges the integrity and functionality of the entire component [2-4].

The key contribution of hydrogen embrittlement (HE) to the SCC behaviors of high-strength Al-Zn-Mg-Cu alloys is increasingly acknowledged [5, 6]. HE can promote the transition from ductile fracture to brittle fracture, including intergranular fracture (IGF) or transgranular quasi-cleavage fracture (QCF) [7, 8]. Better understanding of where the H comes from and how the H triggers the failure of materials are thoroughly needed for HE mitigation. During the SCC test or in practical service, the chemical reactions of the Al substrate with water from the test or service environment are a source of atomic H, a part of which can be subsequently absorbed by the material, referred to as external H [9]. The effects of external H on SCC behaviors of Al-Zn-Mg-Cu alloy have been widely investigated [10, 11]. However, apart from the external H, pre-existing internal H that accumulated during the manufacturing processes [12] may also be involved in the SCC processes; this topic has not yet been deeply explored. The interactions between H and various hydrogen trapping sites, e.g., dislocations [13], vacancies [14], precipitates [1], and second phase particles [16], have been generally reported to be responsible for the occurrence of HE based on hydrogen-enhanced localized plasticity (HELP) [17], hydrogen-enhanced decohesion (HEDE) [18] and adsorption-induced dislocation emission (AIDE) [19]. These works provide a possibility to assess macroscopic fracture behavior based on the distribution of H, taking both external and internal H into consideration, in the SCC of Al-Zn-Mg-Cu alloys. The focus of this study is the elucidation of the contributions of external and internal H to the initiation and propagation of SCC, which is accomplished by combining H-induced nanoscopic debonding and the macroscopic SCC behaviors of a high-strength Al-Zn-Mg-Cu alloy. The results of this study are anticipated to promote an in-depth understanding of the SCC mechanisms of Al-Zn-Mg-Cu alloys and contribute to the suppression of SCC by taking both external and internal H into account.

A high Zn content alloy, Al-9.9Zn-2.3Mg-1.4Cu-0.15Zr-0.06Si-0.05Fe-0.03Ti (wt.%), was prepared on a laboratory scale. An as-rolled Al plate of 13 mm in thickness was subjected to solution treatment at 475 °C for 2 h, followed by water quenching, and a two-stage artificial aging treatment, i.e., initial aging at 120 °C for 6 h and then aging at 150 °C for 5 h, as shown in Fig. S1. Two groups of tensile specimens with low and high internal H contents were sampled along the rolling direction (RD) by electrical discharge machining (EDM) in oil and EDM in oil followed by H charging in humid air at 120 °C for 2 h [1]; H contents were confirmed as 4.5 and 8.3 mass ppm,

respectively, by thermal desorption apparatus. The tensile test was performed *in situ* using a DEBEN CT 500 machine, whilst the entire process was observed by projection-type synchrotron X-ray microtomography (XMT) at the BL20XU undulator beamline in SPring-8. Four experiments were conducted to assess the effects of external and internal H on SCC by changing the test environment, including specimens with high H content tested in distilled water (HW), those with low H content tested in distilled water (LW), those with high H content tested in an Ar atmosphere (HAr), and those with low H content tested in an Ar atmosphere (LAr). Besides, the tensile tests were repeated in the laboratory using completely identical test parameters to achieve a good reproducibility, as described in the supplementary materials. Moreover, 3D finite element method (FEM) simulation was applied to describe the diffusion of external H in the initial stage of HW and LW experiments. The detailed procedures for SCC experiments and simulation are provided in the supplementary materials.

Fig. 1 depicts the nominal stress-strain curves acquired by *in situ* tensile tests and the corresponding fractography observed using SEM. Regardless of the internal H content, the fracture strains were evidently smaller for specimens tested in distilled water compared with those in an Ar atmosphere, indicating that SCC accelerated in the presence of external H from the environment. Moreover, the ductility could also be affected by the internal H content when tests were performed in the same environment. SEM images of the fracture surfaces showed the typical mixed rupture of QCF (highlighted by yellow area) and micro-void coalescence fracture. Su et al. [20] suggested that the areal fraction of QCFs (f_{QCFs}) is an effective indicator for assessing the HE behaviors of the present materials. Calculating the f_{QCF} shows that, regardless of whether the specimen had a low or high internal H content, f_{QCFs} dramatically increased by 3-4 times when the test environment was changed from an Ar atmosphere to distilled water. Most notably, even in a distilled water environment, f_{QCFs} increased by 50% as the internal H content increased. The results seemed to indicate that the contribution of internal H to SCC behavior cannot be neglected despite the crucial role of external H from the environment, and the SCC behavior of Al-Zn-Mg-Cu alloys are controlled by both external and internal H.

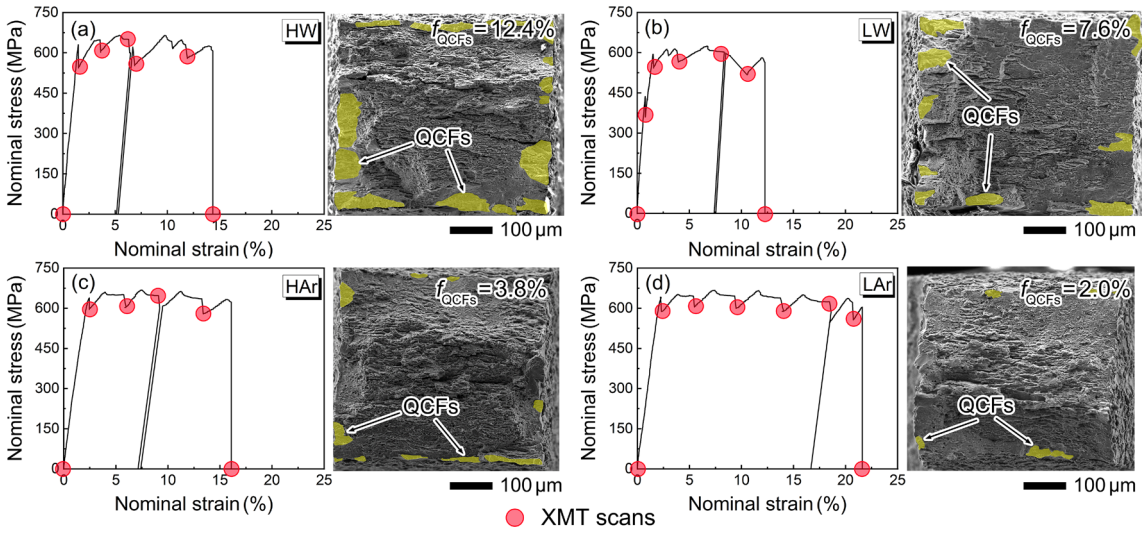

Fig. 1. Nominal stress-strain curves obtained by *in-situ* tensile test and the corresponding SEM morphologies of the fracture surface for (a) HW, (b) LW, (c) HAr, (d) and LAr. The red cycles in the nominal stress-strain curves indicate the operation of XMT scans. The yellow areas in the fracture surface show the distribution of QCFs regions, whose areal fraction (f_{QCFs}) was calculated as 12.4 ± 0.35, 7.6 ± 0.4, 3.8 ± 0.35, and 2.0 ± 0.2% for HW, LW, HAr, and LAr, respectively. The reason why unloading was performed in each experiment is declared in the supplemental materials.

4D observations through projection-type XMT clearly displayed the evolution of QCFs at different applied strains (marked by red cycles in Fig. 1). Fig. 2 clearly demonstrates that all QCFs initiated at the peripheries of the specimens and progressively propagated toward the interior as the applied strain increased. The evolution of the QCF area along with the applied strain for each specimen is quantified in Fig. 3(a). A small number of tiny QCFs with areas of 205, 142 and 47 μm^2 were respectively detected in HW, LW, and HAr after applied strain up to 1.5, 1.5 and 2.5%, whereas LAr remained crack free until the strain reaches 5.5%. Thus, no QCFs were observed in LAr with low internal H content tested in Ar atmosphere after applied strain up to 1.5%. When the internal H content was increased while testing in the same environment (Ar atmosphere), a slight promotion in QCF initiation was observed, as evidenced by the presence of QCFs with areas less than 47 μm^2 in HAr. Notably, when the test environment was shifted from Ar atmosphere to distilled water, the initial QCF area of LW specimens, despite having low internal H content, significantly increased to 142 μm^2. The combination of high internal H and external H further enlarged the QCFs areas to 205 μm^2. These phenomena indicate that both external and internal H facilitated the initiation of QCF, with external H plays a more significant role in the initiation of QCFs. Afterwards, those QCFs appeared to grow continuously and transformed into the propagation stage with increasing strain under the assistance of H. LAr with low internal H contents tested in an Ar atmosphere maintained a constantly small areal fraction of QCFs during the whole tensile process. Moreover, at the same internal H content level, the specimen

tested in distilled water always exhibited a considerably larger area of QCF than that in the Ar atmosphere. Likewise, a high internal H content could promote the propagation of QCFs whether tested in distilled water or an Ar atmosphere. The QCFs in all specimens except LAr, due to its low external and internal H content, propagated at a range of different rates with increasing strain. At the beginning of QCF propagation, each crack shows a relatively low growth rate. As the strain continued to rise, HW and HAr with high internal H contents seem to exhibit higher crack growth rate compared with LW with low internal H contents. Hence, it can be inferred that internal H may contribute to the crack propagation at this stage. With further increasing strain, the crack growth rates exhibited a significant increase, particularly in HW and LW specimens. The aforementioned observations, therefore, suggested that the initiation and propagation of SCC could be significantly accelerated by external H. Interestingly, internal H also played an indispensable role in the SCC of the Al-Zn-Mg-Cu alloy.

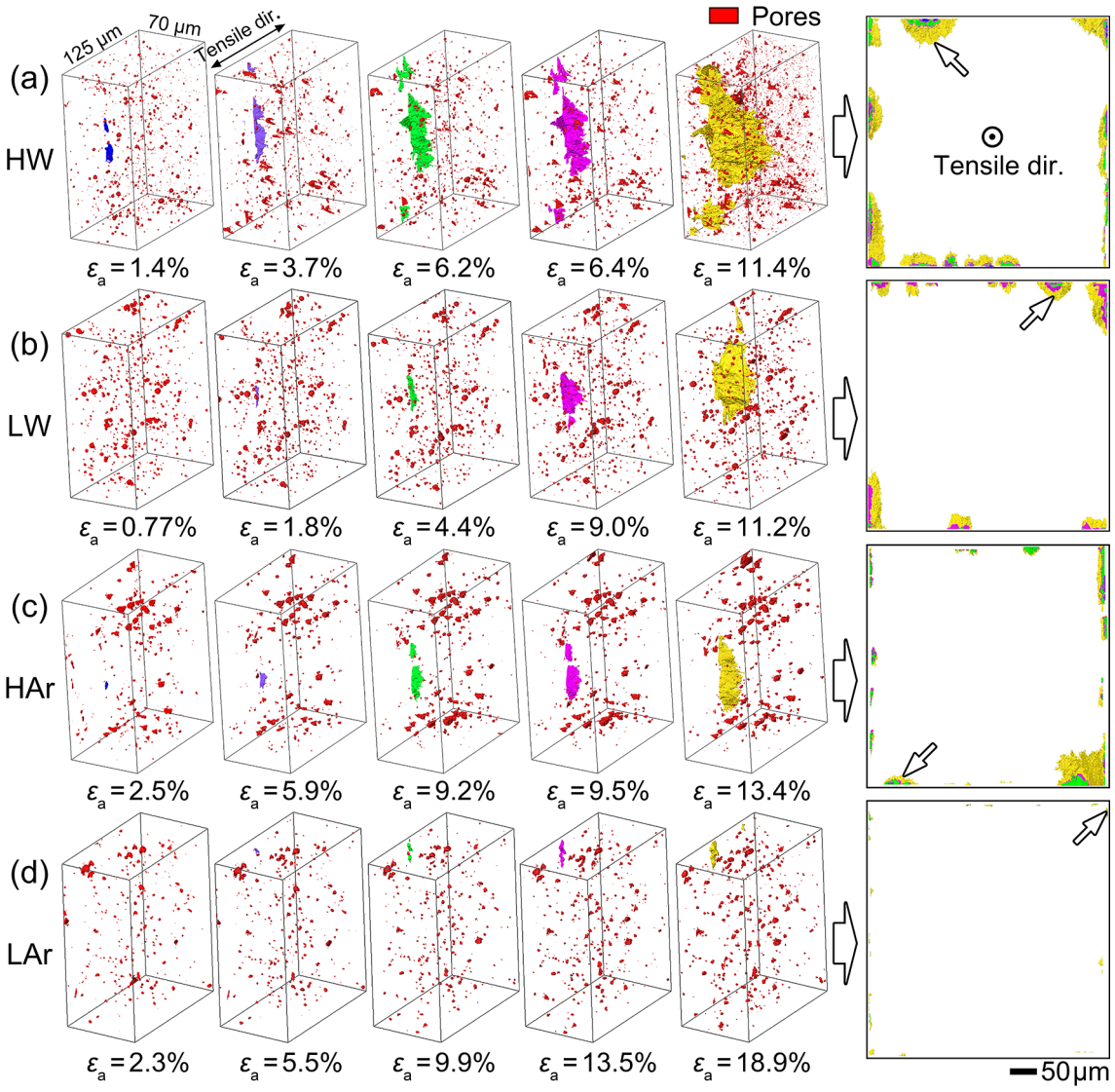

Fig. 2. 3D rendered images of QCFs under different applied strains of (a) HW, (b) LW, (c) HAr and (d) LAr.

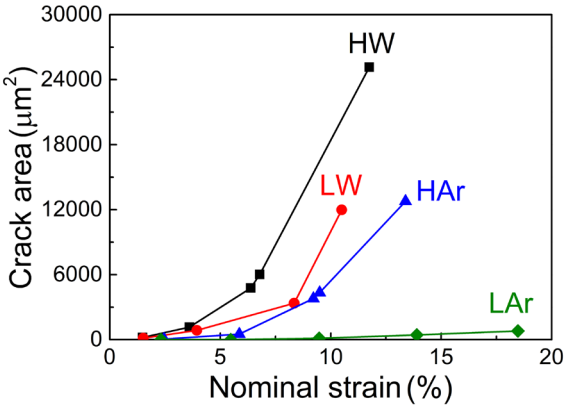

Fig. 3. Variation in total crack area of QCFs distributed on the fracture surface with the applied strain for each specimen.

HE in Al alloys is highly dependent on the interactions between H and the trapping sites [17-19]. Hereinto, either the coalescence of micro-pores or the decohesion of intermetallic particles cannot induce the formation of river-shaped QCFs owing to their large size as well as the large distance between adjacent micro-pores and intermetallic particles [20]. With regard to vacancies, Nagumo, et al. [21] proved the high stability of vacancies where H was trapped, and Su et al. [8] further revealed that repartitioning of H at nanovoids could even enhance the HE resistance of Al-Zn-Mg-Cu alloy. In general, the η-$MgZn_2$ phase is the crucial strengthening precipitate in Al-Zn-Mg-Cu alloys with high Zn content [22]. Moreover, first-principles studies by Tsuru et al. [23] showed that the η-$MgZn_2$/Al interface had a higher H trapping energy and was more likely to trap H than the other trapping sites. They further proposed an unexpected spontaneous fracture process associated with QCF in Al-Zn-Mg alloys because the η-$MgZn_2$/Al interface with high binding energy and high priority of H partitioning could stably trap H at an extremely high occupancy [24]. Fujihara et al. [25] investigated the relationship between the nanoscopic debonding behavior of the η-$MgZn_2$ precipitate and the macroscopic HE behavior during tensile deformation and concluded that QCFs would propagate into the region where the H occupancy of the η-$MgZn_2$ precipitate was greater than 0.31. According to thermal equilibrium theory [26], H repartitioned among different trap sites is in equilibrium with that at normal lattice sites, indicating that the H occupancy in each trap site can be calculated as follows:

$$\frac{\theta_i}{1-\theta_i} = \theta_L \, exp(\frac{E_{b,i}}{RT}) \quad (1)$$

where $E_{b,i}$ is the trap binding energy (Table S2), R is the gas constant (8.31 J $mol^{-1}K^{-1}$), T is the absolute temperature, and θ_L and θ_i are the occupancies of the lattice sites and other trap sites, respectively. Thus, the θ_L was determined as 3.46×10^{-10}. Using θ_L, the H occupancy of dislocations, vacancies, intermetallic particles, precipitates and grain boundaries can be confirmed. Besides, the total H concentration represents the sum of the H stored in the normal lattice sites and all trap sites:

$$C_H^T = \theta_L N_L + \sum \theta_i N_i \quad (2)$$

where C_H^T is the total H concentration, and N_L and Ni are the trap densities in the interstitial lattice and the trap sites (supplementary materials), respectively. In this way, the critical H concentration was calculated as 21 mass ppm to support the H occupancy of the η-$MgZn_2$/Al interface greater than 0.31. This means that QCFs may be more prone to nucleate and propagate in areas where H concentrations are larger than 21 mass ppm, termed as the potential crack region.

The simulated H diffusion behaviors of HW and LW displayed in Fig. 4(a) showed that gradient-distributed H-affected zones with a depth of approximately 30 μm were obtained during the initiation stage. Meanwhile, the internal H was also involved in the formation of these H-affected zones by overlapping with external H. Fig. 4(b) depicts the magnified H distributions near the surfaces of HW and LW, in which the reddish area satisfied the criteria of η-$MgZn_2$ precipitate debonding (H concentration > 21 mass ppm), i.e., regions where there was potential for cracking. Hence, the QCF lengths for HW and LW can be predicted as 5.6 and 4.3 μm, respectively, based on the simulated H distribution. On the other hand, the average lengths of QCFs for HW and LW were calculated as 6.3 and 4.3 μm, respectively, from the XMT images. Apparently, the predicted QCF lengths showed good consistency with the experimental results, indicating that the SCC initiation behaviors of HW and LW can be quantitatively evaluated based on H diffusion behavior. In addition, it is reasonable to infer that H-induced decohesion of η-$MgZn_2$ precipitates in the area where the H concentration was larger than 21 mass ppm provided possible fracture initiation sites for QCF in this study. Gradient-distributed H-affected zones were formed by the uptake and diffusion of external H from the environment, and thus, HW and LW tested in distilled water were more sensitive to SCC. High internal H further increased the area of the potential crack region, making it easier for the HW to initiate QCFs.

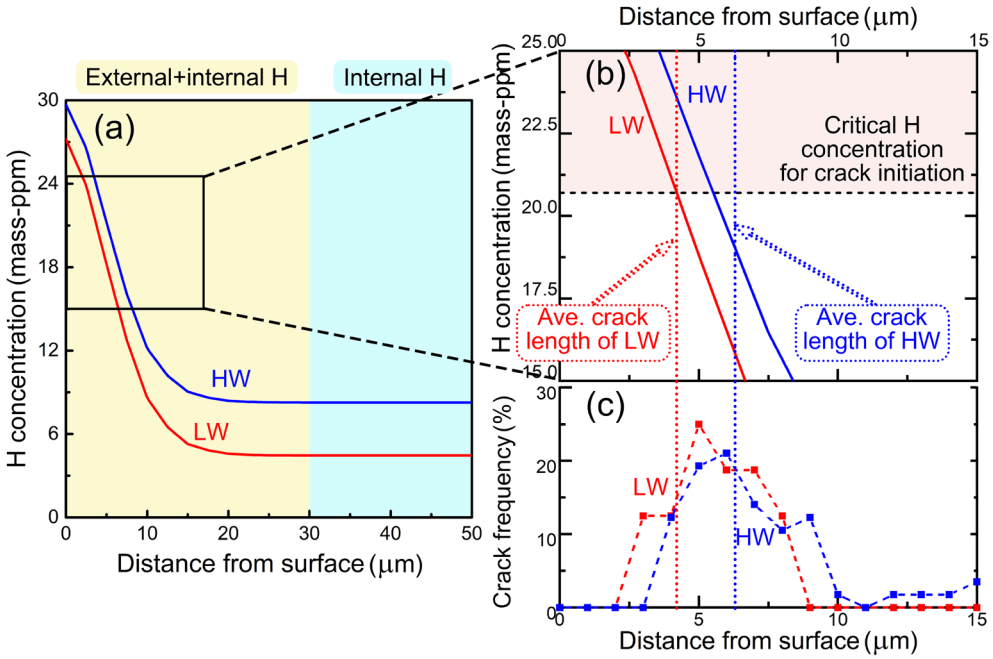

Fig. 4. (a) Simulated result of hydrogen diffusion in HW and LW after exposure to distilled water for 60 min before the first loading, (b) magnified H distribution of HW and LW in the region marked by black rectangle in (a), and (c) distribution of initial crack length.

QCF propagation behaviors should be dependent on the competition between the driving force and the resistance of the local microstructure, which combines coarse intermetallic particles, precipitates and the chemistry at the crack tip [28]. The driving force can be estimated using the stress intensity factor (SIF), which is a function of applied stresses, crack size and component geometry. Notably, the promotion of crack propagation by H was of vital significance during SCC. In the early stage of crack propagation, QCFs with small sizes propagated slowly due to the small driving force. In addition, the potential crack regions near crack tips were not large enough to provide sufficient pathways for crack propagation. Nonetheless, for HW and LW tested in distilled water, cracks grew faster than those tested in an Ar atmosphere due to the larger potential crack region established by external H that had penetrated the material. On the other hand, internal H likely accumulated in the strain localization region ahead of the crack tip under applied stress, leading to localized repartitioning of internal H among various trap sites. During this process, H could preferentially trap in the pores and at the η-$MgZn_2$/Al interface with relatively high binding energy [24, 29]. A larger potential crack region with a higher H concentration could have been formed, where it was easier for them to propagate past those obstacles, leading to HW with a high internal H content exhibiting faster crack growth than LW with a lower internal H content. With continued propagation and opening of cracks, the formation and adsorption of H were facilitated as soon as large areas of bare unpassivated Al surface were exposed to distilled water [30]. Besides, the stress-driven internal H diffusion toward crack tip was continuing,

indicating that a potential crack region with sufficient alternative pathways for crack propagation has been established, thereby cracks tended to sustainably propagate until the specimen failed.

In summary, SCC could initiate and propagate in the potential crack region with an H concentration larger than 21 mass ppm, where the occurrence of nanoscopic H-induced decohesion of η-$MgZn_2$ precipitates resulted in the formation of macroscopic cracks under the synergistic effects of external and internal H. A gradient-distributed H-affected zone was formed by the uptake and diffusion of external H from the environment, which made specimens tested in distilled water more sensitive to SCC. Internal H was driven toward the crack tips during plastic deformation and involved in SCC, making substantial contributions to both the initiation and propagation of cracks.

Acknowledgments

This work was supported by JST, CREST Grant Number JPMJCR 1995 Japan and the Light Metal Educational Foundation. The synchrotron radiation experiments were performed at SPring-8 with the approval of Japan Synchrotron Radiation Research Institute through proposal numbers 2021B1123, 2022A1005 and 2022B1158. The authors would like to thank Mr. Hiroto Motoyama for his contribution to the experiment and data analysis.

References

[1] Y. Wang, B. Sharma, Y. Xu, K. Shimizu, H. Fujihara, K. Hirayama, A. Takeuchi, M. Uesugi, G. Cheng, H. Toda, Switching nanoprecipitates to resist hydrogen embrittlement in high-strength aluminum alloys, Nature Commun. 13 (2022) 6860.

[2] N.J.H. Holroyd, G.M. Scamans, Stress Corrosion Cracking in Al-Zn-Mg-Cu Aluminum Alloys in Saline Environments, Metall. Mater. Trans. A 44 (2013) 1230-1253.

[3] M. López Freixes, X. Zhou, H. Zhao, H. Godin, L. Peguet, T. Warner, B. Gault, Revisiting stress-corrosion cracking and hydrogen embrittlement in 7xxx-Al alloys at the near-atomic-scale, Nature Commun. 13 (2022) 4290.

[4] R.T. Euesden, Y. Aboura, A.J. Garner, T. Jailin, C. Grant, Z. Barrett, C. Engel, P. Shanthraj, N.J.H. Holroyd, P.B. Prangnell, T.L. Burnett, In-situ observation of environmentally assisted crack initiation and short crack growth behaviour of new-generation 7xxx series alloys in humid air, Corros. Sci. 216 (2023) 111051.

[5] R.G. Song, W. Dietzel, B.J. Zhang, W.J. Liu, M.K. Tseng, A. Atrens, Stress corrosion cracking and hydrogen embrittlement of an Al-Zn-Mg-Cu alloy, Acta Mater. 52 (2004) 4727-4743.

[6] L. Wang, J. Liang, H. Li, L. Cheng, Z. Cui, Quantitative study of the corrosion evolution and stress corrosion cracking of high strength aluminum alloys in solution and thin electrolyte layer containing Cl, Corros. Sci. 178 (2021) 109076.

[7] M.L. Martin, B.P. Somerday, R.O. Ritchie, P. Sofronis, I.M. Robertson, Hydrogen-induced intergranular failure in

nickel revisited, Acta Mater. 60 (2012) 2739-2745.

[8] H. Su, H. Toda, R. Masunaga, K. Shimizu, H. Gao, K. Sasaki, M.S. Bhuiyan, K. Uesugi, A. Takeuchi, Y. Watanabe, Influence of hydrogen on strain localization and fracture behavior in Al-Zn-Mg-Cu aluminum alloys, Acta Mater. 159 (2018) 332-343.

[9] S.P. Knight, K. Pohl, N.J.H. Holroyd, N. Birbilis, P.A. Rometsch, B.C. Muddle, R. Goswami, S.P. Lynch, Some effects of alloy composition on stress corrosion cracking in Al-Zn-Mg-Cu alloys, Corros. Sci. 98 (2015) 50-62.

[10] H. Kamoutsi, G.N. Haidemenopoulos, V. Bontozoglou, S. Pantelakis, Corrosion-induced hydrogen embrittlement in aluminum alloy 2024, Corros. Sci. 48 (2006) 1209-1224.

[11] Y. Aboura, A.J. Garner, R. Euesden, Z. Barrett, C. Engel, N.J.H. Holroyd, P.B. Prangnell, T.L. Burnett, Understanding the environmentally assisted cracking (EAC) initiation and propagation of new generation 7xxx alloys using slow strain rate testing, Corros. Sci. 199 (2022) 110161.

[12] Q. Han, S. Viswanathan, Hydrogen evolution during directional solidification and its effect on porosity formation in aluminum alloys, Metall. Mater. Trans. A 33 (2002) 2067-2072.

[13] J. Song, W.A. Curtin, Atomic mechanism and prediction of hydrogen embrittlement in iron, Nature Mater. 12 (2013) 145-151.

[14] J. Hou, X.S. Kong, X. Wu, J. Song, C.S. Liu, Predictive model of hydrogen trapping and bubbling in nanovoids in bcc metals, Nature Mater. 18 (2019) 833-839.

[15] A.K. Zurek, R. Walser, H.L. Marcus, Deuterium transport and trapping in aluminum alloys, Metall. Mater. Trans. A 14 (1983) 1307-1312.

[16] Y. Wang, H. Toda, Y. Xu, K. Shimizu, K. Hirayama, H. Fujihara, A. Takeuchi, M. Uesugi, In-situ 3D observation of hydrogen-assisted particle damage behavior in 7075 Al alloy by synchrotron X-ray tomography, Acta Mater. 227 (2022) 117658.

[17] C.D. Beachem, A new model for hydrogen-assisted cracking (hydrogen “embrittlement”), Metall. Trans. 3 (1972) 441-455.

[18] R. Oriani, A mechanistic theory of hydrogen embrittlement of steels, Acta Mater. 76 (1972) 848-857.

[19] S.P. Lynch, Environmentally assisted cracking: Overview of evidence for an adsorption-induced localised-slip process, Acta Mater. 36 (1988) 2639-2661.

[20] H. Su, H. Toda, K. Shimizu, K. Uesugi, A. Takeuchi, Y. Watanabe, Assessment of hydrogen embrittlement via image-based techniques in Al-Zn-Mg-Cu aluminum alloys, Acta Mater. 176 (2019) 96-108.

[21] M. Nagumo, Hydrogen related failure of steels - a new aspect, Mater. Sci. Technol. 20 (2004) 940-950.

[22] S.J. Won, H. So, L. Kang, S.J. Oh, K.H. Kim, Development of a high-strength Al-Zn-Mg-Cu-based alloy via multi-strengthening mechanisms, Scr. Mater. 205 (2021) 114216.

[23] T. Tsuru, M. Yamaguchi, K. Ebihara, M. Itakura, Y. Shiihara, K. Matsuda, H. Toda, First-principles study of hydrogen segregation at the $MgZn_2$ precipitate in Al-Mg-Zn alloys, Comp. Mater. Sci. 148 (2018) 301-306.

[24] T. Tsuru, K. Shimizu, M. Yamaguchi, M. Itakura, K. Ebihara, A. Bendo, K. Matsuda, H. Toda, Hydrogen-accelerated spontaneous microcracking in high-strength aluminium alloys, Sci. Rep. 10 (2020) 1998.

[25] H. Fujihara, H. Toda, K. Ebihara, M. Kobayashi, T. Mayama, K. Hirayama, K. Shimizu, A. Takeuchi, M. Uesugi, Assessment of hydrogen embrittlement behavior in Al-Zn-Mg alloy through multi-modal 3D image-based simulation, Acta Mater. Under review (2023) http://dx.doi.org/10.2139/ssrn.4523623.

[26] R.A. Oriani, The diffusion and trapping of hydrogen in steel, Acta Mater. 18 (1970) 147-157.

[27] L. Wen, W. Liu, G. Wu, H. Wu, L. Zhang, J. Sun, J. Zhang, S. Xu, C. Shi, Y. Wang, Y. Lu, Microstructure and stress corrosion cracking resistance of Al-6.5Zn-2Cu-1.5Mg-0.05Ti alloy modified by Cr addition, Mater. Charact. 183 (2022) 111621.

[28] V.C. Gudla, M. Storm, B.C. Palmer, J.J. Lewandowski, P.J. Withers, N.J.H. Holroyd, T.L. Burnett, Environmentally induced crack (EIC) initiation, propagation, and failure: A 3D in-situ time-lapse study of AA5083 H131, Corros. Sci. 174 (2020) 108834.

[29] M. Dadfarnia, M.L. Martin, A. Nagao, P. Sofronis, I.M. Robertson, Modeling hydrogen transport by dislocations, J. Mech. Phys. Solids 78 (2015) 511-525.

[30] Z. Xu, P. Zhang, B. Zhang, B. Lei, Z. Feng, Y. Shao, Y. Wang, G. Meng, Effect of tensile stress on the hydrogen adsorption of X70 pipeline steel, Int. J. Hydrogen Energy 47(50) (2022) 21582-21595.